

¹ **Photobleaching of Red**

² **Fluorescence in Oral Biofilms**

³ **C. K. Hope,^{*1} E. de Josselin de Jong,^{1,2}, M. R. T. Field,³ S. P.**

⁴ **Valappil,¹ and S. M. Higham¹**

⁵

⁶ **¹School of Dental Sciences, University of Liverpool, UK**

⁷ **²Inspektor Research Systems BV, Amsterdam, Netherlands**

⁸ **³Department of Human Anatomy and Cell Biology, University of Liverpool, UK**

⁹

¹⁰ ***Corresponding Author:** Dr Chris Hope, University of Liverpool, School of Dental

¹¹ Sciences, Research Wing, Daulby Street. United Kingdom, L69 3GN. Tel: +44(0) 151 706

¹² 5296 Email: chope@liv.ac.uk

¹³

¹⁴ **Key Words:**

¹⁵ Oral biofilm, plaque, fluorescence, quantitative light-induced fluorescence digital (QLFD),

¹⁶ porphyrin, photobleaching

¹⁷

¹⁸

19 **Abstract**

20 *Background and Objective:* Many species of oral bacteria can be induced to fluoresce due
21 to the presence of endogenous porphyrins, a phenomenon that can be utilised to visualise
22 and quantify dental plaque in the laboratory or clinical setting. However; an inevitable
23 consequence of fluorescence is photobleaching, and the effects of this on longitudinal,
24 quantitative analysis of dental plaque has yet to be ascertained.

25 *Material and Methods:* Filter membrane biofilms were grown from salivary inocula or single
26 species (*Prevotella nigrescens* and *Prevotella intermedia*). The mature biofilms were then
27 examined in a custom-made lighting rig comprising of 405 nm light emitting diodes capable
28 of delivering 220 W m^{-2} at the sample, an appropriate filter and a digital camera; a set-up
29 analogous to quantitative light-induced fluorescence digital (QLFD). Longitudinal sets of
30 images were captured and processed to assess the degradation in red fluorescence over
31 time.

32 *Results:* Photobleaching was observed in all instances. The highest rates of
33 photobleaching were observed immediately after initiation of illumination, specifically during
34 the first minute. Relative rates of photobleaching during the first minute of exposure were;
35 19.17, 13.72, and 3.43 (arbitrary units per minute) for *P. nigrescens* biofilms, microcosm
36 biofilm and *P. intermedia* respectively.

37 *Conclusion:* Photobleaching could be problematic when making quantitative measurements
38 of porphyrin fluorescence *in situ*. Reducing both light levels and exposure time, in
39 combination with increased camera sensitivity, should be the default approach when
40 undertaking analyses by QLFD.

41 **Introduction**

42 **Porphyrins and oral bacteria**

43 Fluorescent porphyrins are present in many members of our indigenous microbiota (1, 2),
44 including those found in the oral cavity (3-5). Whilst many bacterial porphyrins are
45 associated with photosynthesis, a relatively large amount of haem (iron protoporphyrin IX)
46 for example is incorporated on the cell surface of the putative periodontal pathogen
47 *Porphyromonas gingivalis* to protect it from hydrogen peroxide (6) with similar processes
48 occurring in *Prevotella nigrescens* and *Prevotella intermedia* (7) (both formerly classified as
49 *Bacteroides melanogenicus*) (8) . The molecular fluorescence of bacterial porphyrins is an
50 adventitious phenomenon which results from the absorption of a photon and the subsequent
51 re-emission of another photon of a longer wavelength as the electrons in the molecule return
52 from the excited (triplet) state to the ground state. Specific porphyrins have distinct
53 excitation spectra with different maxima; protoporphyrin at 593 nm and coproporphyrin 604
54 nm (9). The wavelengths suitable for the efficient fluorescent excitation of bacterial
55 porphyrins range from near ultraviolet (300 nm) to blue (450 nm). The discrepancy between
56 the colour of the incident light and the fluorescent emission, a phenomenon known as the
57 Stokes shift (10), allows for the selective capture and quantification of the emitted light via an
58 appropriate filter set-up.

59 Photobleaching occurs when a fluorophore is irreversibly damaged so that it no longer
60 fluoresces. Although the exact mechanisms by which photobleaching occur are not clear, it
61 has been suggested that the fluorophores undergo an oxidative reaction with highly reactive
62 oxygen species such as singlet oxygen (${}^1\text{O}_2$) and hydroxyl radicals (OH^-) (11). Molecules
63 already in the excited (singlet) state can also be destructively excited by an additional
64 excitation photon, an event dubbed two-photon excitation, but it is unlikely that this process
65 would occur in the experiments discussed herein. Other results have demonstrated
66 photobleaching reactions occurring between excited dye molecules (12) . The generation of

67 highly reactive oxygen species has also been demonstrated to cause cell death in *P.*
68 *gingivalis*, *P. nigrescens* and *P. intermedia* by the excitation of endogenous porphyrins (13).
69 Lethal photosensitisation (photodynamic therapy) either by the application of
70 photosensitising agents or via endogenous porphyrins has the potential to be an effective
71 means of treating plaque-related diseases (14) .

72 Fluorescence microscopy techniques can utilise the kinetics of photobleaching by
73 fluorescence loss in photobleaching (FLIP) and fluorescence recovery after photobleaching
74 (FRAP) to reveal rates of diffusion within cell membranes, organelles (15) and biofilms (16).
75 However, when undertaking quantitative measurements of fluorescence, photobleaching can
76 be problematic (17). A better understanding of photobleaching phenomena with respect to
77 indigenous bacterial porphyrins *in situ* is required to enable accurate quantitative analyses of
78 dental plaque to be undertaken.

79

80 **Quantitative light-induced fluorescence**

81 Quantitative Light-induced Fluorescence (QLF) uses violet light to induce fluorescence in
82 tooth enamel and collects the resulting emissions via a high band-pass filter (>520 nm) in
83 conjunction with a computer-controlled digital camera (18). When viewed under QLF lighting
84 conditions, areas of demineralised enamel fluoresce less than surrounding sound enamel
85 and so appear darker. Regions of demineralised enamel are visible under QLF lighting
86 conditions before they are visible to the eye as white spot lesions (19). Although QLF was
87 initially developed for the analysis of tooth enamel (20), it has been subsequently
88 demonstrated to be capable of revealing dental plaque due to the fluorescence of
89 endogenous porphyrins (5). Quantitative Light-Induced Fluorescence Digital (QLFD) is an
90 adaptation of QLF which employs a modified filter set (D007, Inspektor Research Systems
91 BV, Amsterdam, Netherlands), narrow-band violet light (405 nm) and a high-specification
92 digital SLR camera. This configuration has been specifically developed to enhance the

93 visualisation and quantification of plaque. During clinical investigations to assess plaque,
94 QLFD is typically used to identify regions of red fluorescence and capture a sequence of
95 images at different visits in order to quantify the progression of conservative dental
96 treatment.

97 **Materials and Methods**

98 **Filter membrane biofilms**

99 Approximately 10 ml of unstimulated saliva was obtained from a healthy volunteer with no
100 previous history of periodontitis. This was split into 1 ml aliquots and frozen. Nitrocellulose
101 filter-membranes (47 mm diameter, 0.45 µm pore size, Invitrogen Ltd., Paisley,
102 Renfrewshire, UK) were laid, with their inked grid upwards, on top of blood agar (Oxoid,
103 Basingstoke, UK) supplemented with 5% defibrinated horse blood. A 50 µl aliquot of the
104 saliva sample was spread over the membrane before being incubated at 37°C in anaerobic
105 conditions (80% N₂, 10% CO₂, 10% H₂) for seven days to allow microcosm oral biofilms to
106 develop. Individual biofilm laden filter membranes were removed from the supporting agar
107 and placed in a Petri dish which had first had 200 µl of phosphate buffered saline (PBS)
108 beaded over the surface to help prevent the membrane biofilm from drying out. Similar
109 single-species biofilms were grown using heavy colony inocula of *Prevotella nigescens*
110 (ATCC 25261) (seven day old cultures) or *Prevotella intermedia* (ATCC 25611) (five day old
111 cultures) suspended in 1 ml of PBS.

112

113 **Fluorescence imaging**

114 A custom-made rig, incorporating QLFD technology, was constructed to enable the capture
115 of fluorescent images under reproducible lighting conditions from surface-mounted indium
116 gallium nitride light emitting diodes (LED) (EWC 400 SC2C, radiant power 600 mW, 23°
117 beam angle; E Wave Corporation, London, UK) with a wavelength band from 400 nm to a

118 peak output at 405 nm (violet). To construct the QLFD *in vitro* rig, an LED was soldered
119 onto the outside of a copper ring, being a section of standard domestic plumbing material,
120 which acted as a heat-sink to prevent overheating. Three such mounted LEDs were then
121 fixed inside an approximately hemispherical plastic bowl so that the light beams converged
122 on the sample (Figure 1). A hole was cut into the base for the unimpeded viewing of the
123 sample by a camera, with another hole in the sidewall to allow the sample to be easily
124 manipulated. The LEDs were powered by a DC adaptor with an output of 5 volts at 1.2
125 amps connected in parallel. The distance between the LEDs and the sample was 100 mm
126 at an angle of incidence between camera and LEDs of 30° from the surface normal. The
127 light incident on the sample was measured as irradiance by a photosynthetically active
128 radiometer (PAR) with a cosine corrected detector (Q201 PAR with SD221Q Cos detector,
129 Macam Photometrics Limited, Livingston, UK). A cut-off filter (D007, Inspektor Research
130 Systems BV, Amsterdam, Netherlands) was placed in front of the camera lens to minimise
131 the transmission of light close to the excitation wavelength whilst maximising the
132 transmission of the red part of the spectrum. All illumination / photobleaching experiments
133 were undertaken in a dark-room.

134 Images were captured with a ‘live view’ enabled digital SLR camera, (Model: 1000D, Canon,
135 Tokyo, Japan) equipped with a 60 mm, f/2.8 macro lens (Model: EF-S, Canon) connected to
136 a computer. Proprietary software (C2 v1.0.0.7, Inspektor Research Systems BV) was used
137 to control the camera and store the images. Low apertures (i.e. f/2.8 to f/8) and ISO settings
138 of 200 – 400 were typically used to maximise the light sensitivity of the camera without
139 adversely affecting image quality. The camera’s on-board ‘custom white balance’ feature
140 was calibrated against a sheet of white paper before fluorescence imaging to effectively
141 eliminate the colouration of the filter in the resulting images. The camera resolution was set
142 to ‘low’ (3.4 megapixels) to facilitate the processing of large numbers of data files in the form
143 of uncompressed 24-bit bitmap files. The LEDs were switched on for at least 10 minutes
144 prior to use to allow their temperature to stabilise. Without moving the sample, or changing

145 camera settings, a series of images was captured over time using the in-built image
146 sequencer incorporated into the control software. Control experiments included membranes
147 that were partially covered with aluminium foil to shield portions of them from the light. Four
148 separate microcosm biofilm photobleaching experiments were undertaken whilst the
149 experiments for single species were conducted in duplicate.

150

151 **Image analysis**

152 Images were analysed with an open source software package (ImageJ 1.43q, The National
153 Institutes of Health, Bethesda, Maryland, USA, <http://rsb.info.nih.gov/ij/>). The images
154 comprising the time-lapse sequence were opened with ImageJ and compiled into a single
155 image 'stack'. The stack was then split into its red, green and blue (RGB) component colour
156 channels; to isolate the red channel as an 8-bit greyscale (i.e. pixel brightness values from 0
157 to 255). A user-defined 'rectangular selection' region of interest (ROI) was created within
158 one of the inked grid squares on the filter membrane. The size of the grid squares was 4
159 mm x 4 mm and the ROI encompassed approximately 20 000 pixels. The 'z-axis profile' of
160 the ROI was then measured through the image stack and the mean pixel brightness values
161 at each time point were copied into Microsoft Excel. The ROI was then moved to an
162 adjacent square on the grid and the process repeated to give a total of eight discrete counts
163 from the same biofilm sample. The mean pixel brightness values from the eight sample
164 sights from the were then themselves averaged before being normalised to 100 at time zero
165 to yield the arbitrary unit used throughout these experiments; 'normalised mean pixel
166 brightness' (NMPB), which allowed the direct comparisons to be made between separate
167 experiments.

168 Changes in fluorescence (ΔF) were calculated in terms of the shift in NMPB per unit time to
169 yield results in terms of ΔF per minute. These ΔF values were then allocated into sub-sets
170 to determine mean ΔF between discrete time points within the photobleaching experiment;
171 from 0 to 1 minute, 1 to 2 minutes, 2 to 5 minutes, 5 to 10 minutes and 10 to 20 minutes.

172

173 **Inter-operator reliability**

174 Two researchers (CKH and MRTF) independently analysed the image stacks from two
175 photobleaching experiments in order to ascertain the reliability of the methods previously
176 described. This exercise was undertaken in light of the possible variability due to manual
177 selection of the ROI parameters; namely: size of ROI, placement of ROI within the
178 membrane square and choice of the eight membrane squares used for analysis. Results
179 were tested using Pearson Correlation with PASW Statistics 17.0 (equivalent to SPSS)
180 (Polar Engineering and Statistics).

181

182 **Results**

183 **Light exposure**

184 The configuration of the LEDs at an angle of incidence to the sample of 30° (Figure 1)
185 corresponded to a radiant intensity of 0.87 per unit solid angle (Lambert's cosine law). The
186 angle of incidence was within the angular response parameters of the cosine corrected PAR
187 detector. The maximum radiometer reading at the sample location was 750 $\mu\text{mol m}^{-2} \text{s}^{-1}$,
188 which is equivalent to 220 W m^{-2} at 405 nm. Light leakage from the LEDs was minimal,
189 being measured at 1.8 $\mu\text{mol m}^{-2} \text{s}^{-1}$ immediately outside the obvious pool of light from a
190 single LED. Due to the build-up of heat during operation, the LED's light output dropped to
191 89% of their initial power after 10 minutes usage after which time their output stabilised (data
192 not shown).

193

194 **Biofilm photobleaching**

195 Photobleaching was evident in all of the samples analysed in this study; microcosm oral
196 biofilm, *P. nigrescens* and *P. intermedia* single-species biofilms. A control experiment was
197 designed to confirm that light was responsible for the reduction in fluorescence in which half
198 of the sample was shielded from direct illumination with aluminium foil. After 25 minutes, the
199 NMPB on the exposed half dropped to 31.23 whilst the covered half was 84.73 (figure 2).

200 Figure 3 shows the results from an individual QLFD experiment which demonstrates
201 photobleaching as a decrease in NMPB over time. NMPB data such as these were collated
202 to yield means along with their corresponding standard deviations (Figure 4).

203 Rates of photobleaching, expressed as ΔF were highest during the initial stages of exposure
204 to light (i.e. the first minute). In the case of microcosm biofilms and *P. nigrescens* biofilms,
205 photobleaching rates fell to approximately half their initial value after 10 minutes exposure
206 (Figure 5). Initial rates of photobleaching during the first minute of exposure, expressed as
207 ΔF (arbitrary units normalised to 100 at time zero) per minute, were; 19.17, 13.72, and 3.43
208 for *P. nigrescens* biofilms, microcosm biofilm and *P. intermedia* respectively.

209 Photobleaching dynamics were reproducible between replicate samples; Pearson correlation
210 coefficient values between the four microcosm biofilm samples ranged from 0.993 to 0.997
211 and were significant at the 0.01 level (2-tailed).

212

213 **Inter-operator reliability**

214 Pearson correlation coefficients for the two photobleaching experiments subjected to inter-
215 operator reliability testing were significant at the 0.01 level (2-tailed) with correlations of
216 0.992 and 1. The data presented herein was the first set of data that was analysed.

217

218 **Discussion**

219 **Light exposure**

220 A PAR detector was chosen to measure the light irradiance from the custom rig since
221 photobleaching is dependent on the amount of light energy incident per unit surface area
222 and not the power output of the LEDs *per se* (21). The camera / image analysis method of
223 quantifying pixel brightness proved far more sensitive to subtle changes in ambient lighting
224 conditions than the results from the PAR detector would have suggested. The data collected
225 from the automated image sequencer yielded fewer perturbations in the fluorescence curve
226 than when captured manually during preliminary experiments. This suggested that variation
227 in lighting from the laptop screen, reflected off the white laboratory coat worn by the
228 operator, was detectable in the analysed images. The inter-operator reliability data suggests
229 that the image analysis methods employed were robust and reproducible.

230 Whilst every effort was made to focus the light onto the centre of the filter membrane, an *ad-*
231 *hoc* observation made using the PAR revealed that a single representative attempt to place
232 the detector in the ‘bright centre of the light beams’ by the unaided eye, yielded only 73% of
233 the actual maximum irradiance obtainable by scrutinising the meter readings. The difference
234 between these two positions was of the order of 10 mm. Although the foci of the LEDs were
235 generally convergent onto the sample, it is unclear how the extent of photobleaching relates
236 to specific positions within the pool of light incident on the sample. For example, an area
237 with less light incident upon it, will fluoresce less and will likewise have a lower rate of
238 photobleaching (22). The net result of this would be differential rates of photobleaching
239 across a (large) sample and a hypothetical example of this effect is demonstrated in Figure
240 6. Performing image analysis on adjacent sites on the biofilm membrane will help to
241 minimise the effects of heterogeneous lighting. Another confounding factor that should be
242 considered is the photo-shielding effect (23) which occurs when a relatively high
243 concentration of fluorophore absorbs excitation photons, which in turn reduces the number

244 of photons able to penetrate into deeper layers of the sample. ‘Iron porphyrin’ can account
245 for up to 50% of the dry weight of the biomass of *Bacteroides* (many of which have been
246 reclassified as *Prevotella spp.*) when growing on blood agar (24) . Photo-shielding could
247 reduce the observed effects of photobleaching due to decreased excitation within the sample
248 as a whole; in other words, there may not be a direct relationship between fluorescence
249 intensity / photobleaching and net porphyrin concentration within a heterogeneous, three-
250 dimensional microbial biofilm.

251

252 **Biofilm photobleaching**

253 Rates of photobleaching decreased during exposure to QLFD light for 20 minutes, after
254 which time there was very little further reduction in observed fluorescence. It is unlikely that
255 imaging (exposure) times beyond this would be representative of image capture *in vivo*. A
256 reduction in mean pixel brightness of ~14% after one minute’s illumination with QLFD
257 represents an unacceptable inaccuracy for the quantitative analysis of the red fluorescence
258 of dental plaque. Casual viewing and manipulation of a sample / patient under the 405 nm
259 lighting in order to correct the focus, determine other camera settings and image capture will
260 inevitably cause photobleaching. In order to minimise this effect, samples should be
261 positioned and focussed under normal, white-light conditions. It is however an unavoidable
262 fact that in order to observe fluorescence, one must perturb fluorescence.

263 The rates of ΔF observed suggest that this effect was immediate and replicated the
264 photobleaching kinetics of protoporphyrin IX previously observed in PLC hepatoma cells at
265 405 nm (25). In the current study, ΔF values were grouped to yield average values for all
266 data points within discrete time bands (0 to 1 minutes, 1 to 2 minutes, 2 to 5 minutes, 5 to 10
267 minutes and 10 to 20 minutes) to obviate the confounding effects of individual data points
268 with a positive ΔF value amongst predominantly negative ΔF (i.e. fluorescence decreasing)
269 values. During a longitudinal study, a system whereby the LEDs are only illuminated during

270 imaging should be employed. This will also maximise the power output of the LEDs as they
271 emit more light when they are at ambient (room) temperature as opposed to once they have
272 warmed to their operating temperature. Using the PAR detector it was determined that the
273 irradiance supplied by the lighting rig did not decrease due to heating effects when operated
274 for 5 seconds out of every minute, similarly lighting for 5 seconds out of every 30 seconds
275 only reduced light output to 99.45% (data not shown).

276 The differential fluorescence of oral anaerobic bacteria under ultraviolet light has been
277 suggested as a tool for their rapid identification. The fluorescence previously observed in
278 strains of *Bacteroides* (now reclassified as *Prevotella spp.* and *P. gingivalis*) encompasses a
279 colour range that has been described as; red, yellow, red-orange, brilliant red, pink-orange,
280 orange, yellow-orange, and red-brown (26) . These colours also changed with age of the
281 culture and are almost certainly a manifestation of the sequential metabolism of porphyrins
282 (27) . No fluorescence was observed in *P. gingivalis* at any time, including when emulsified
283 in methanol – a technique which can reveal fluorescence in older cultures which have lost
284 this capacity (2) . The inability of *P. gingivalis* to fluoresce is probably due to the deposition
285 of haem as an μ -oxo dimer on the cell surface, as opposed to the monomeric form in
286 *Prevotella* (6, 7). It was observed in preliminary experiments that the fluorescence of *P.*
287 *intermedia* was greatly diminished when incubated for seven days, hence the use of younger
288 (five day) cultures.

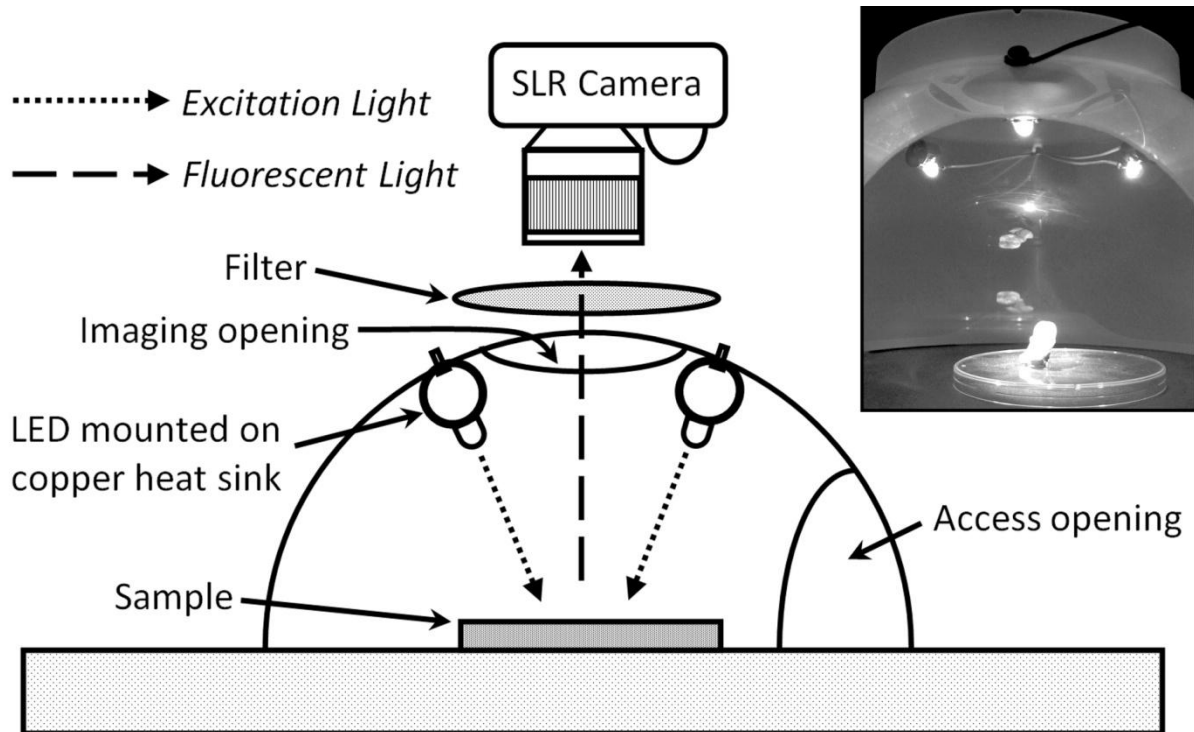
289 Fluorescence imaging has the potential to be a useful tool for quantifying dental plaque in
290 the research environment (28). The methodology described herein for measuring
291 photobleaching of red fluorescence in microbial biofilms appears to be robust and
292 reproducible. However; the destruction of the endogenous fluorophores within dental plaque
293 by photobleaching phenomena needs to be considered and steps taken to curtail this effect
294 in both the research and clinical environments such as improving camera sensitivity, filter
295 characteristics and keeping irradiance to a minimum.

296 **Acknowledgments**

297 This work was undertaken as a final year research project by MRTF and was funded
298 internally by the University of Liverpool, School of Dental Sciences and Department of
299 Human Anatomy and Cell Biology.

300

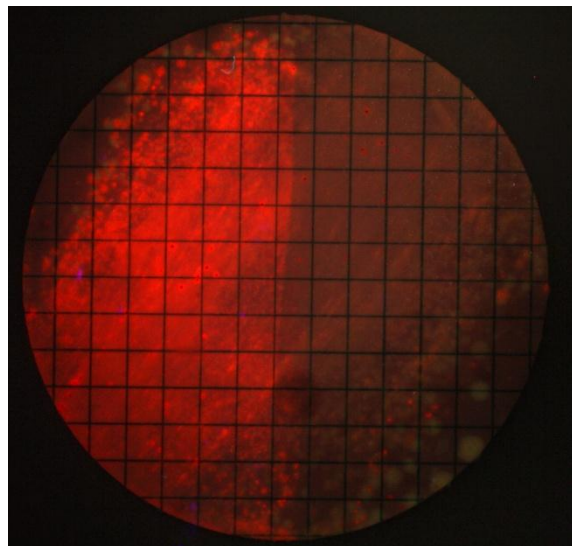
301 **Figures**



302

303 Figure 1. Schematic diagram of the 405 nm lighting rig, comprising of three equidistant
304 indium gallium nitride light emitting diodes (inset: a tooth sample illuminated by the lighting
305 rig).

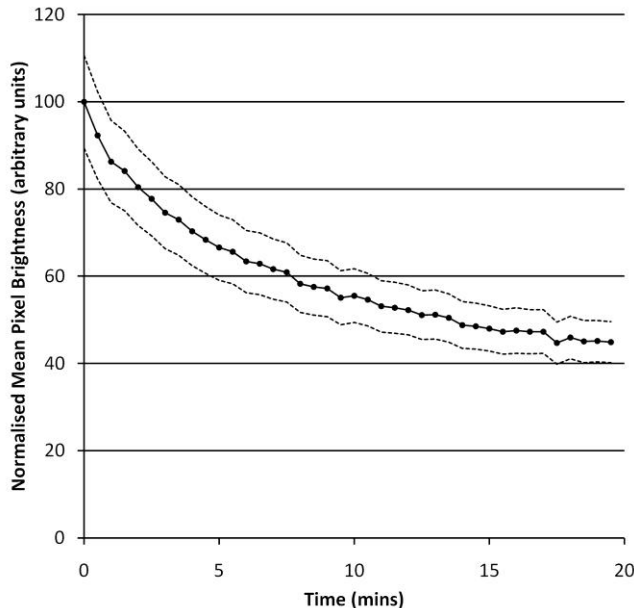
306



307

308 Figure 2. Microcosm filter-membrane biofilm viewed under the QLFD lighting system.
309 Photobleaching was demonstrated on the right-hand side of the membrane in this instance
310 by previously covering the left-hand side of the membrane with aluminium foil whilst 405 nm
311 light at $750 \mu\text{mol m}^{-2} \text{s}^{-1}$ (maximum) was incident onto the sample for 25 minutes. The foil
312 was removed immediately before this image was captured.

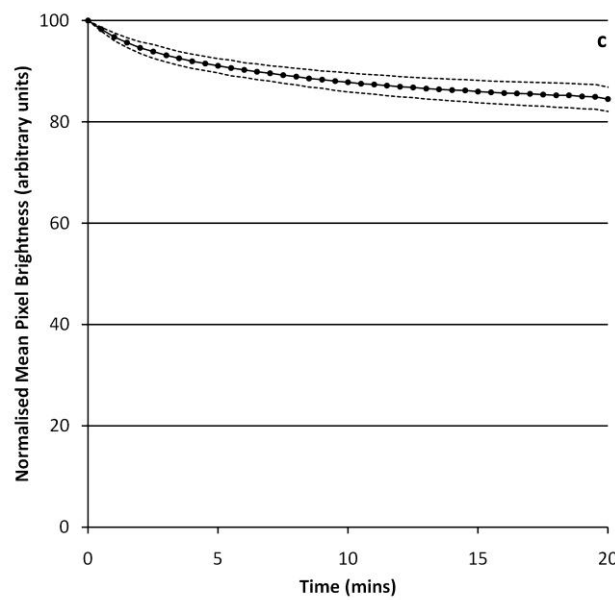
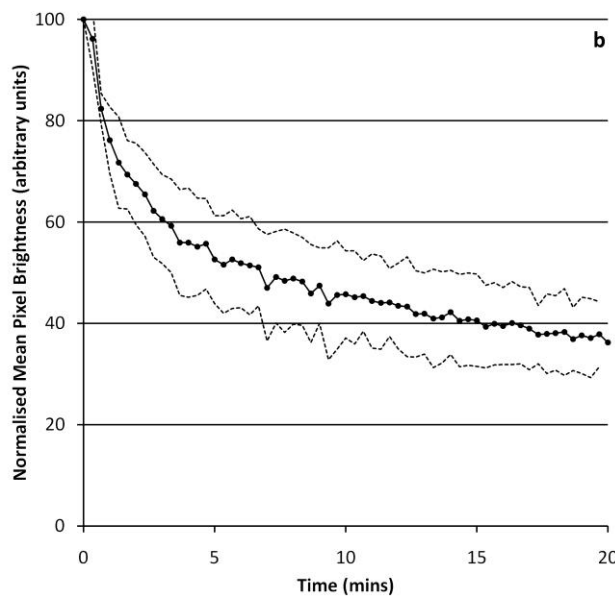
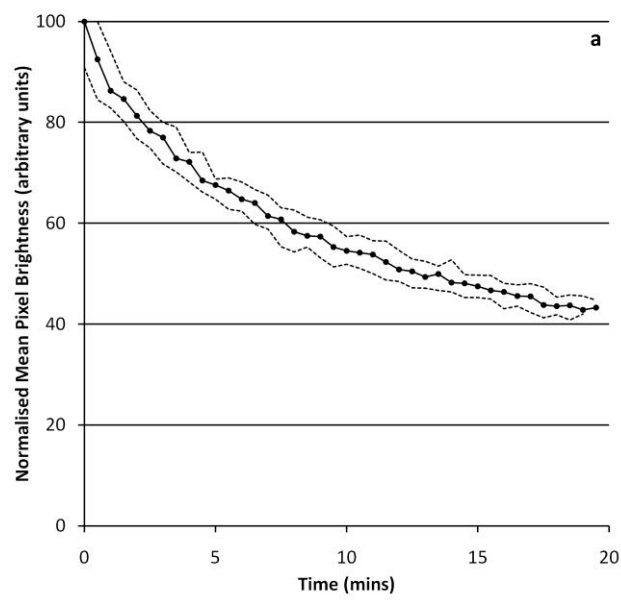
313



314

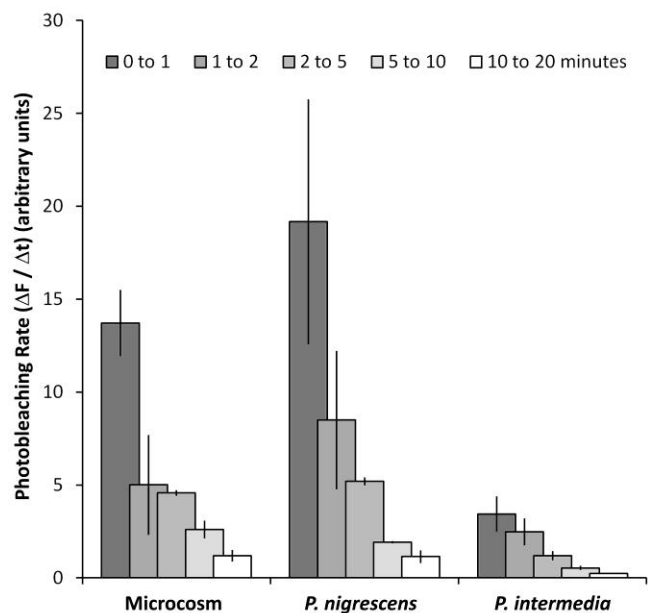
315 Figure 3. A representative microcosm biofilm photobleaching experiment following
316 illumination with the QLFD lighting system. The solid line is the mean pixel brightness from
317 adjacent regions of interest within the sample ($n=8$); the dotted lines show standard
318 deviations.

319



321 Figure 4. Mean red fluorescence observed in microcosm (n=4) (a), *P. nigrescens* (n=2) (b)
322 and *P. intermedia* (n=2) (c) filter-membrane biofilms viewed under QLFD lighting. The solid
323 lines represent the mean values with the dotted lines showing standard deviations.

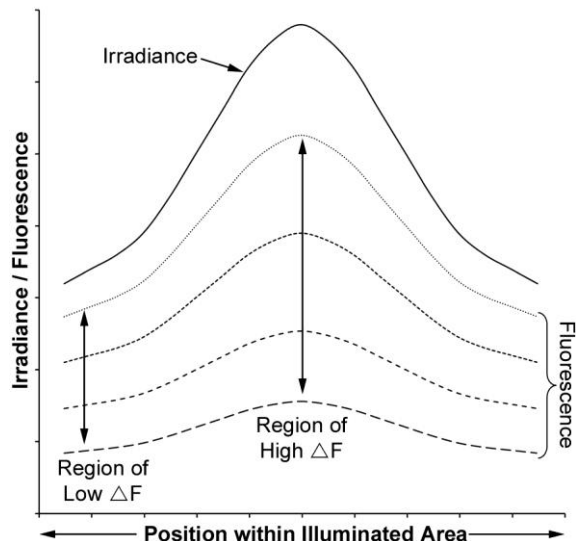
324



325

326 Figure 5. Rates of photobleaching shown as the decrease in fluorescence (ΔF) with time
 327 (Δt) within a range of time points; 0 to 1, 1 to 2, 2 to 5, 5 to 10 and 10 to 20 minutes. These
 328 data corresponds to Figure 4. Error bars indicate standard deviations.

329



330

331 Figure 6. A theoretical model showing differential rates of photobleaching across a sample
 332 illuminated with the custom lighting rig. Heterogenous irradiance of the sample is
 333 represented by the solid line, whereas the resulting fluorescence values are shown by the
 334 dotted lines at four times points. Fluorescence decreases over time and the rate of
 335 photobleaching is directly proportional to the incident irradiation.

336

337 **References**

- 338 (1) McGinley KJ, Webster GF, Leyden JJ. Facial follicular porphyrin fluorescence:
339 correlation with age and density of Propionibacterium acnes. *BrJDermatol*
340 1980; **102**: 437-441.
- 341 (2) Myers MB, Cherry G, Bornside BB, Bornside GH. Ultaviolet red fluorescence
342 of Bacteroides melaninogenicus. *Appl Microbiol* 1969; **17**: 760-762.
- 343 (3) Chow AW, Patten V, Guze LB. Rapid screening of Veillonella by ultraviolet
344 fluorescence. *J Clin Microbiol* 1975; **2**: 546-548.
- 345 (4) Lennon AM, Buchalla W, Brune L, Zimmermann O, Gross U, Attin T. The
346 ability of selected oral microorganisms to emit red fluorescence. *Caries Res*
347 2006; **40**: 2-5.
- 348 (5) Coulthwaite L, Pretty IA, Smith PW, Higham SM, Verran J. The
349 microbiological origin of fluorescence observed in plaque on dentures during
350 QLF analysis. *Caries Res* 2006; **40**: 112-116.
- 351 (6) Smalley JW, Birss AJ, Silver J. The periodontal pathogen Porphyromonas
352 gingivalis harnesses the chemistry of the mu-oxo bishaem of iron
353 protoporphyrin IX to protect against hydrogen peroxide. *FEMS Microbiol Lett*
354 2000; **183**: 159-164.
- 355 (7) Smalley JW, Silver J, Birss AJ, Withnall R, Titler PJ. The haem pigment of the
356 oral anaerobes Prevotella nigrescens and Prevotella intermedia is composed
357 of iron(III) protoporphyrin IX in the monomeric form. *Microbiology* 2003; **149**:
358 1711-1718.
- 359 (8) Shah HN, Collins DM. Prevotella, a new genus to include Bacteroides
360 melaninogenicus and related species formerly classified in the genus
361 Bacteroides. *Int J Syst Bacteriol* 1990; **40**: 205-208.
- 362 (9) Lin DL, He LF, Li YQ. Rapid and simultaneous determination of
363 coproporphyrin and protoporphyrin in feces by derivative matrix isopotential
364 synchronous fluorescence spectrometry. *Clin Chem* 2004; **50**: 1797-1803.
- 365 (10) Stokes GG. On the Change of Refrangibility of Light. *Philosophical
Transactions of the Royal Society of London* 1852; **142**: 463-562.
- 366 (11) Tong-Sheng CS-Q, Z.; Wei, Z.; Qing-Ming, L. A quantitative theory model of a
367 photobleaching mechanism. *Chinese Physics Letters* 2003; **20**: 1940-1943.
- 368 (12) Song L, Varma CA, Verhoeven JW, Tanke HJ. Influence of the triplet excited
369 state on the photobleaching kinetics of fluorescein in microscopy. *Biophys J*
370 1996; **70**: 2959-2968.
- 371 (13) Soukos NS, Som S, Abernethy AD, et al. Phototargeting oral black-pigmented
372 bacteria. *Antimicrob Agents Chemother* 2005; **49**: 1391-1396.
- 373 (14) Wilson M. Lethal photosensitisation of oral bacteria and its potential
374 application in the photodynamic therapy of oral infections.
PhotochemPhotobiolSci 2004; **3**: 412-418.
- 375 (15) Koster M, Frahm T, Hauser H. Nucleocytoplasmic shuttling revealed by FRAP
376 and FLIP technologies. *Curr Opin Biotechnol* 2005; **16**: 28-34.
- 377 (16) Bryers JD, Drummond F. Local macromolecule diffusion coefficients in
378 structurally non-uniform bacterial biofilms using fluorescence recovery after
379 photobleaching (FRAP). *Biotechnol Bioeng* 1998; **60**: 462-473.
- 380 (17) Hope CK, Wilson M. Induction of lethal photosensitization in biofilms using a
381 confocal scanning laser as the excitation source. *J Antimicrob Chemother*
382 2006; **57**: 1227-1230.

- 385 (18) de Josselin de JE, Sundstrom F, Westerling H, Tranaeus S, ten Bosch JJ,
386 ngmar-Mansson B. A new method for in vivo quantification of changes in
387 initial enamel caries with laser fluorescence. *Caries Res* 1995; **29**: 2-7.
388 (19) Gmur R, Giertsen E, van dV, de Josselin de JE, Ten Cate JM, Guggenheim
389 B. In vitro quantitative light-induced fluorescence to measure changes in
390 enamel mineralization. *ClinOral Investig* 2006.
391 (20) Ando M, Hall AF, Eckert GJ, Schemehorn BR, Analoui M, Stookey GK.
392 Relative ability of laser fluorescence techniques to quantitate early mineral
393 loss in vitro. *Caries Res* 1997; **31**: 125-131.
394 (21) McCree KJ. Significance of Enhancement for Calculations Based on the
395 Action Spectrum for Photosynthesis. *Plant Physiol* 1972; **49**: 704-706.
396 (22) Patterson GH, Piston DW. Photobleaching in two-photon excitation
397 microscopy. *Biophys J* 2000; **78**: 2159-2162.
398 (23) Herzog M, Moser J, Wagner B, Broecker J. Shielding effects and hypoxia in
399 photodynamic therapy. *IntJOral MaxillofacSurg* 1994; **23**: 406-408.
400 (24) Rizza V, Sinclair PR, White DC, Cuorant PR. Electron transport system of the
401 protoheme-requiring anaerobe *Bacteroides melaninogenicus*. *J Bacteriol*
402 1968; **96**: 665-671.
403 (25) Lu S, Chen JY, Zhang Y, Ma J, Wang PN, Peng Q. Fluorescence detection of
404 protoporphyrin IX in living cells: a comparative study on single- and two-
405 photon excitation. *J Biomed Opt* 2008; **13**: 024014.
406 (26) Slots J, Reynolds HS. Long-wave UV light fluorescence for identification of
407 black-pigmented *Bacteroides* spp. *J Clin Microbiol* 1982; **16**: 1148-1151.
408 (27) Shah HN, Bonnett R, Mateen B, Williams RA. The porphyrin pigmentation of
409 subspecies of *Bacteroides melaninogenicus*. *Biochem J* 1979; **180**: 45-50.
410 (28) Pretty IA, Edgar WM, Smith PW, Higham SM. Quantification of dental plaque
411 in the research environment. *JDent* 2005; **33**: 193-207.
- 412
413